ELSEVIER

Journal of Chromatography A, 917 (2001) 179–185

JOURNAL OF CHROMATOGRAPHY A

www.elsevier.com/locate/chroma

Characterization of starch polysaccharides by flow field-flow fractionation–multi-angle laser light scattering–differential refractometer index

P. Roger[a,b], B. Baud[a], P. Colonna[a,*]

[a]*Institut National de la Recherche Agronomique, rue de la Géraudière, BP 71627, 44316 Nantes Cedex 03, France*
[b]*Lab. de Chimie Organique Multifonctionnelle, Université Paris-Sud, Bat. 420, F-91405 Orsay Cedex, France*

Received 18 August 2000; received in revised form 5 February 2001; accepted 22 February 2001

Abstract

The coupling between flow field-flow fractionation (FFF), multi-angle laser light scattering and differential refractometer index provides a promising technique for fractionation of starch polysaccharides in aqueous conditions. Native starches with different amylose/amylopectin levels (0–70%) as well as a pure amylose sample were characterized. By applying a sudden drop in the cross-flow-rate, clear separation was achieved between amylose (which elutes first) and amylopectin. Flow FFF produced correct relationships between the molecular mass or the gyration radius versus elution volume for the fractionated amylopectin population. The results are also considered in terms of the macromolecular composition of starches.

Keywords: Starch; Polysaccharides; Amylose; Amylopectin

1. Introduction

Starch is an insoluble granule in cold water. It consists of a mixture of two alphaglucans (i.e. polysaccharide made of the same monomer unit, the anhydro-glucose residue) containing mainly alpha-(1,4) linkages. Whereas amylose (AMY) is essentially linear, amylopectin (AMP) is branched with 5–6% alpha-(1,6) linkages. They also have different weight-average molar masses, radii of gyration and hydrodynamic radii ($\bar{M}_w$~10^5–10^6 g/mol, $\bar{R}_G$~10–60 nm and $\bar{R}_H$~10–30 nm for AMY [1] and $\bar{M}_w$~2×10^8 g/mol and $\bar{R}_G$~$\bar{R}_H$ 200 nm for AMP [2]).

Due to the very high size of the AMP component, the available HPSEC columns could be considered to be useless due to the too low exclusion limit in the high molar mass range of those columns.

However it has been shown [3] that a quantitative elution profile of starch in water can be obtained by high-pressure liquid chromatography if appropriate solubilisation and chromatographic conditions are used.

Before running a separation technique, care has to be taken with starches in order to assess a complete dissolution in the eluent, which was not done until recently. Starch samples were dissolved directly in water at high temperature (140–150°C) under pres-

*Corresponding author. Fax: +33-24-067-5006.
E-mail addresses: ph.roger@icmo.u-psud.fr (P. Roger), colonna@nantes.inra.fr (P. Colonna).

0021-9673/01/$ – see front matter
PII: S0021-9673(01)00689-6

sure using a procedure which allowed complete dissolution [3].

The recovery of starch after the chromatographic elution has also to be assessed which is also generally not the case in most of the papers dealing with the subject.

By using silica gel based columns with low porosity it has been shown that starch recovery is quantitative and that the experimental profiles can be explained by the combined effect of hydrodynamic chromatography (HDC) and size exclusion chromatography (SEC) [4]. Some further improvements are needed in order to obtain a better resolution between AMP and AMY peaks.

It is the aim of this work to test the efficiency of field flow fractionation in the high molar mass range [5] for starch characterisation. Practically FFF works if one flux perpendicular to the main elution direction is added. The main usual fluxes are temperature gradient, gravitation or crossflow. To our knowledge only few works involving those FFF techniques have been reported for starch characterisation until now. A partial separation of starch polymers has been obtained [6] by using thermal FFF and DMSO as solvent. It has also been shown [7] that sedimentation FFF was adapted for waxy maize (i.e. a 100% AMP level) characterisation in aqueous condition. The problem of this technique is that the exclusion limit in the lower size range is too low to fractionate below approximately 50 nm. Then starch profiles will always be truncated of the amylose component.

First results of starch polysaccharides fractionation using the coupling between crossflow FFF, multiangle laser light scattering (MALLS) and a differential refractometer index (DRI) are presented here.

2. Material and methods

2.1. Material

Corn starches with different AMY contents (0, 30, 50 and 70%) as well as pure synthetic amylose have been studied. The corn starches were a gift from a french starch producer (Roquette Frères, Lestrem, France). There were waxy (0% AMY content) and normal (30% AMY content) corn starches and two high amylose rich starches (50 and 70% AMY content, respectively). The synthetic amylose was obtained from maltohexaose (DP6) by enzymatic polymerisation [8]. It is referred to as sample S6 in that reference and was characterised by SEC–MALLS using pure water as solvent (M_w=4.8×10^5 g/mol and R_G~22.5 nm). Starch is first dissolved in a 95% DMSO/water binary solvent, precipitated with alcohol, washed and dried. It is then redissolved in water at high temperature (140–150°C) under pressure using microwave heating [3] leading to a solubilisation extent of 91–99%.

2.2. Methods

Starch solutions (0.5 mg/ml, 70 μl) are filtrated through 5 μm durapore membranes (Waters, Bedford, USA), except the amylose solution which is filtrated through a lower porosity (0.45 μm) membrane. The solutions are then directly injected into a flow FFF–MALLS–DRI set-up. The flow FFF instrument is the 1000-FISI model (FFFractionation Inc., Salt Lake City, Utah, USA). The channel of the flow FFF is symmetrical with a frit outlet. The semi-permeable membrane is made of regenerated cellulose (cut off: 10 000 g/mol). The channel dimensions are 250 μm×30 cm×2.5 cm.

The two on-line detectors are a multiangle light scattering instrument, the Dawn® DSP-F, fitted with a KS flow cell and a He–Ne laser, (λ=632.8 nm), from Wyatt Technology Corp. (Santa Barbara, USA) and a refractometer (ERC-7515, Erma, Tokyo, Japan) using a tungsten filament as a light source emitting visible radiations. The mobile phase (Millipore water containing 0.02% sodium azide) is eluted initially at a flow-rate of 1 ml/min for channel flow in. In parallel a frit outlet flow-rate was fixed to 0.5 ml/min to increase the signal at the detectors which decreases the flow-rate of the channel flow out down to 0.5 ml/min. The flow-rate of the crossflow is maintained at 0.6 ml/min until a retention volume of 5.6 ml for all the samples (except for normal corn starch where this retention volume was 5 ml) and decreased stepwise down to 0.1 ml/min until the end of the elution peak (10–11 ml).

Sample recoveries are obtained from the ratio of the mass eluted from the channel (integration of the DRI signal with (dn/dc) of the polymer sample and DRI calibration constant which are known) and the

injected mass. The injected mass is obtained by the sulphuric acid — orcinol colorimetric method [9].

2.3. Data treatment

After treatment of the LS and DRI profiles using the ASTRA® software from WTC (version 1.4 for Macintosh), the quantities c_i, M_i, and R_{Gi} which are respectively the mass concentration, molar mass, and mean square radius of the ith slice were obtained. M_i and R_{Gi} are obtained at each slice of the chromatogram peak using the Berry extrapolation method. The Berry extrapolation method is used instead of the well-known Zimm extrapolation because it allows a more accurate extrapolation in the case of very high radius of gyration [10].

Weight-average molar mass M_w and z-average root-mean-square (rms) radii of gyration R_G in nm were then calculated by using the summations taken over one peak.

A value of 0.146 ml g^{-1} [11] was employed as refractive index increment (dn/dc). An interdetector delay volume of 175 μl was determined by injecting BSA-monomer Sigma Chemical Co., Poole, U.K.) i.e. a purified bovine serum albumin sample with a narrow molar mass distribution. Normalization of the photodiodes was obtained using the P20 pullulan standard (Showa Denko K. K., Tokyo, Japan) of molar mass, 410 g/mol.

3. Results and discussion

On the LS (for a scattering angle of 900) and DRI profiles of all the samples (Fig. 1A,B) a void peak appears systematically at an elution volume V_e~2.5 ml. The fact that the injected sample solution contains no azide contrary to the mobile phase could explain the DRI signal but in any case the LS response at the same elution volume. The void peak probably contains a fraction of the polymer sample which will be shown to be a minor fraction below.

3.1. DRI profiles

In the case of starch samples containing a mixture of AMP and AMY i.e. 30% AMY, 50% AMY and 70% AMY, the DRI profiles are bimodal (Fig. 1B).

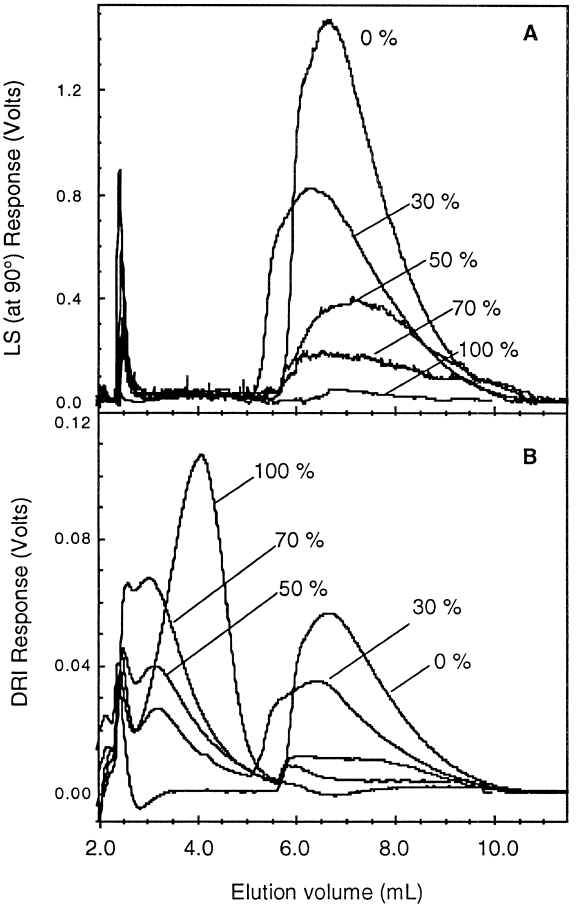

Fig. 1. Light scattering (A) and DRI (B) profiles of the five starch samples. The labels correspond to the percentage of AMY content.

A first peak elutes beginning at the void peak (2.5 ml) and ending at 5–6 ml. For the 0% AMY content starch solution, no DRI response was observed in this first elution volume range. It can be also noticed that the peak area of this peak increases in the order of the AMY content. The top of this first peak is situated at V=3.2, 3.3 and 3.4 ml for 70% AMY, 50% AMY and 30% AMY, respectively. That increase in elution volume indicates a first difference in macromolecular features with a probable slight increase of the amylose dimension (i.e. both M_w and R_H) as the amylose content decreases. However the difference in elution volume is so small that it has to be checked by a reproducibility study as the present results were obtained by injecting the majority of the samples only one time. The synthetic amylose sam-

ple elutes in the same elution range i.e. 2.5–6 ml but the profile is quite different with a peak maximum obtained for an elution volume of 4.1 ml. That difference in dimension was expected as the synthetic amylose sample is strictly linear whereas the amylose population of starch contains branch points, decreasing its hydrodynamic size for a given molar mass.

The second macromolecular peak is located between elution volumes of 5–6 ml and 11 ml. The level of the DRI response increases with the AMP content of the sample. The second peak for normal corn starch (30% AMY content) begins to elute sooner than in the case of the three other starch samples containing AMP because the condition of the elution is different: the decrease of the crossflow-rate was applied sooner. It gives no additional information to compare the peak maxima in those conditions.

So due to the known difference in size between AMY (hydrodynamic radius between 10 and 30 nm) and AMP (R_H~200 nm) but also due to the relative increase in the two peak height compared with the relative content of the two components, the first peak can be identified without any doubt to be amylose and the second one to represent amylopectin.

A clear separation is obtained on the DRI profiles between AMY and AMP. Sample recoveries of 84–100% are obtained meaning that the response is almost quantitative for all the starches and the synthetic amylose sample.

In those conditions, it is meaningful to calculate from the integration of the two peaks area the respective proportion of AMY and AMP in the starch samples containing those two components. The integration of the first peak corresponds to 28%, 68% and 83% of the total area for 30% AMY, 50% AMY and 70% AMY respectively. Those percentages are higher than the amylose content obtained using iodine binding capacity (IBC) which are 27%, 50% and 67% amylose content respectively. Those differences can be explained considering that starch can contain a third component (INT) with an intermediate structure between amylose and amylopectin (it has a lower molar mass and higher average chain length of the repeating units between branching points than AMP, but higher molar mass and lower average chain length than AMY). That third starch component has been already characterised in a high amylose content starch at a level of 13% [12,13]. In normal starches it is considered that the third component is missing or represents a minor fraction [12]. That could explain the similar amylose content obtained by integration of the first peak area for the 30% AMY starch. However it's possible to observe an inflexion point at 4.1 ml on the DRI profiles of all the starch samples which contain amylose (30% AMY, 50% AMY and 70% AMY). The position of this inflexion point is obtained from the deviation of the straight line corresponding to the tangent d*(DRI)*/dV_1 after the top of the amylose peak. It divides the amylose peak into two fractions (Fig. 2). Percentages of peak area of the third component corresponding to the peak area after the inflexion point are 5, 17 and 14% for 30% AMY, 50% AMY and 70% AMY samples, respectively. Then for the AMY-rich starches the remaining fraction correspond to 51 and 69% which is similar or very close to the values obtained by IBC, respectively 51 and 67% for 50% AMY and 70% AMY samples. When IBC is used, only amylose chain with chain length having a degree of polymerisation higher than 100 are taken into account. That explains why the third component is considered to be amylopectin-like by IBC. All those numerical values have to be considered with caution because of possible uncertainties in the calculation of the total area due to (1) baseline

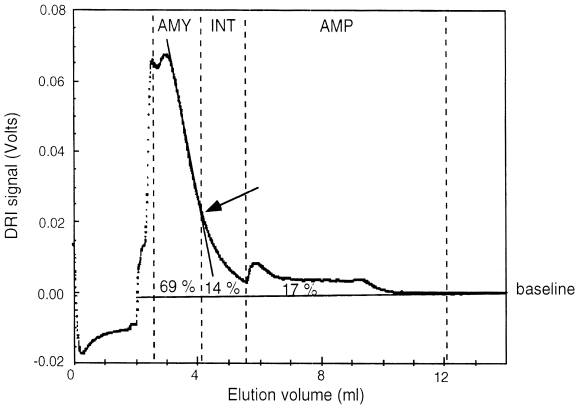

Fig. 2. DRI profile of 70% AMY sample with the baseline and the corresponding area of the different polymers of starch (AMY, amylose; INT, intermediate material; AMP, amylopectin). The position of the inflexion point is indicated by an arrow. See text for further details.

fluctuation, (2) the presence of the unresolved void peak at 2.5 ml, and (3) the present lack of reproducibility study. For example, if the void peak is included in the calculation of the 100% area then the percentages of population change to 74% (AMY population), 12% (intermediate population) and 14% (AMP population). So a maximum deviation of 5% deviation occurs compared if the area is calculated without the void peak (Fig. 2).

3.2. LS profiles and average values of molar mass and radius of gyration

Whereas for amylopectin LS signals are high enough, the signal-to-noise ratio is not big enough to characterize with precision the AMY population of the starch samples (Fig. 1A).

For the pure amylose sample, the LS signal-to-noise ratio is low but it allows to calculate a $\bar{M}_w$ value of $(4.8\pm1.3)\times10^5$ g/mol which is not significantly different from the value of $(4.3\pm0.3)\times10^5$ g/mol obtained by SEC–MALLS [8].

Results of weight average molar masses and *z*-average radii of gyration are of the same order (Table 1) as those obtained by performing static light scattering alone [2].

3.3. R_{Gi} and M_i versus elution volume curves and structural information for the amylopectin population

For the amylopectin population, both the radius of gyration and the molar mass increase with the elution volume (Fig. 3). Those experimental curves are going to be explained and studied to extract some structural information.

In flow FFF, there is a direct relationship between

Table 1
Weight-average molar mass and *z*-average radius of gyration of the four starches as obtained after integration of the whole profile

AMY content (%)	$\bar{M}_w$ (g/mol)	$\bar{R}_G$ (nm)
0	4.5×10^8	334
30	1.3×10^8	205
50	3.6×10^7	144
70	3.2×10^7	112

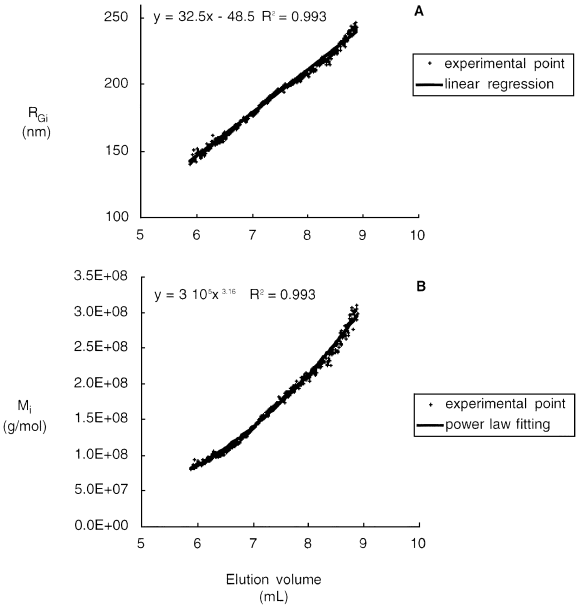

Fig. 3. R_{Gi} and M_i versus elution volume V_i curves for the amylopectin population of the 30% AMY content starch sample (i.e. normal corn starch).

the elution time t_{ri} (or the retention time $R_t = t_{ri}/t^0$ where t^0 is the void time) and the inverse of the translational coefficient of diffusion D_i [5]:

$$R_i = \frac{t_{ri}}{t^0} = \frac{w}{6l_i} = \frac{|u_0|w}{6D_i} \quad (1)$$

where w is the channel thickness and l_i is the distance from the centre of gravity of the sample zone to the accumulation wall for a rentention time t_{ri}, $|u_0|$ is the velocity of the crossflow close to the ultrafiltration membrane. This equation is already approximated considering an efficient separation when $w \gg l_i$.

The proportionality between t_i and R_{Hi} is obtained using the well known Stoke–Einstein equation:

$$D_i = \frac{kT}{6\pi\eta R_{Hi}} \quad (2)$$

where k is the Boltzmann's constant, T the temperature, and η the viscosity of the solvent.

So:

$$R_i = \frac{t_{ri}}{t^0} = \frac{|u_0|w\pi\eta}{kT} R_{Hi} \quad (3)$$

If the polymer structure is analogous all along the distribution, then the ratio between the radius of gyration and the hydrodynamic radius can be considered to be constant in a first approximation. This ratio is usually known as the ρ-factor in the literature [14]:

$$\rho = R_{Gi}/R_{Hi} \quad (4)$$

The ρ-factor depends on the polymer structure: $\rho =$ 0.778 for a sphere, $\rho = 1.5$ for a random coil under θ conditions, $\rho = 1.78$ for a random coil in a good solvent and $\rho > 2$ for a rod. Practically for a highly branched polymer, it is considered that $\rho < 1.5$ and for linear polymer $\rho \geq 1.5$. For AMP, ρ-factor values in the range 1–1.5 have been obtained [2]. So if ρ has a constant value all along the AMP peak one should obtain a linear relationship between RGI and V_i as it is observed in Fig. 3A.

Now to explain the molar mass increase with the elution volume (Fig. 3B) it's necessary to introduce the molar mass dependence of polymer chain dimensions in dilute solutions. Semi-empirical power laws of the Mark–Houwink–Sakurada type have been established both theoretically [15–17] and experimentally [8,18,19] using either R_{Gi} or R_{Hi}:

$$R_{Gi} = K_G M_i^{\upsilon_G} \quad (5)$$

$$R_{Hi} = K_H M_i^{\upsilon_H} \quad (6)$$

The exponents ν_G and ν_H depend on polymer shape, polymer–solvent interactions and temperature.

For example, $\nu_G = \nu_H = 0.33$ for a sphere, $\nu_G = \nu_H =$ 0.5–0.6 for a monodisperse linear random coil and $\nu_G = \nu_H = 1$ for a monodisperse rod.

So by combining Eqs. (3) and (6), it is found that the molar mass M_i versus the retention time t_{ri} relation is a power law equation:

$$M_i = \left(\frac{|u_0| w \pi \eta}{t^0 kT}\right)^{1/\nu_H} (t_{ri})^{1/\upsilon_H} \quad (7)$$

To use elution volume V_i instead of retention time, t_{ri} is replaced in Eq. (7) by $V_i/\mathrm{FR} = 2V_i$ where FR = flow-rate = 0.5 ml/min.

The coefficient ν_H is obtained either from the inverse of the slope of the linear regression of the double logarithmic plot of the molar mass versus elution volume or directly by fitting the experimental data points (M_i, V_i), to the power law Eq. (7) (Fig. 3B). In both cases, by using the data points corresponding to the AMP peak of the 30% AMY content sample, a very good fit is obtained and the value of the power-law exponent $\nu_H = (3.16)^{-1} = 0.32$ is very close to the value of 0.33 calculated for a hard-sphere model.

In Fig. 4 are shown the log–log plots of R_{Gi} vs. M_i for the four starch samples. The ν_G-values of Eq. (5) are usually obtained from the corresponding slope.

For the AMP rich starches (0 and 30% AMY) the straight-lines obtained are nearly undistinguishable with a ν_G-value of 0.40 in agreement with previous studies [2,3,7].

For a flexible and linear polymer like amylose the exponent VG is in the range 0.5–0.6 depending on the solvent quality [8]. Here the presence of branching in amylopectin decreases the ν value. It can also be concluded that the structures of the AMP population are identical for the two AMP rich starches.

For the two AMY rich starches, it is not possible to obtain the slope because of the strong curvature. The experimental R_{Gi} vs. M_i curves are below the curves obtained for the AMP rich starches. That could be the indication of a higher density of the amylopectin component of the AMY rich starches

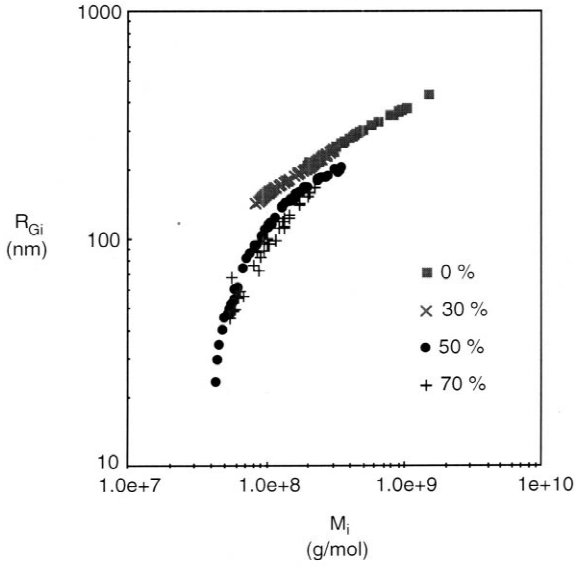

Fig. 4. Log–log plot of R_{Gi} vs. M_i for the amylopectin population.

but it is necessary to increase the LS signals to noise ratio to conclude definitely on that point.

Then once again [2] significant differences between the power-law exponents ν_G and ν_H are experimentally obtained for the branched structure of amylopectin.

4. Conclusion

The fractionation of starch polysaccharides using flow FFF is promising. It leads to a better peak resolution as compared to recent results obtained by HDC–SEC. However some further developments are still needed in order to characterise the complete molecular mass distribution in addition to the AMP fraction.

Acknowledgements

The authors thank SOPARES (Gentilly, France) for the loan during one week of the FFF equipment and one of its staff member (Thierry Azoulay) for his skillful help during the experiments.

References

[1] P. Roger, P. Colonna, Int. J. Biol. Macromol. 19 (1996) 51.
[2] P. Roger, L.A. Bello-Pérez, P. Colonna, Polymer 40 (1999) 6897.
[3] L.A. Bello-Pérez, P. Roger, B. Baud, P. Colonna, J. Cereal Sci. 27 (1998) 267.
[4] B. Baud, Ph.D. Thesis (1999) University of Nantes.
[5] J.C. Giddings, Science 260 (1993) 1456.
[6] J. Lou, M.N. Myers, J.C. Giddings, J. Liq. Chromatogr. 17 (1994) 3239.
[7] R. Hanselmann, W. Burchard, M. Ehrat, H.M. Widmer, Macromolecules 29 (1996) 3277.
[8] P. Roger, M.A.V. Axelos, P. Colonna, Macromolecules 33 (2000) 2446.
[9] V. Planchot, P. Colonna, L. Saulnier, in: B. Godon, W. Loisel (Eds.), Guide Pratique d'Analyses dans les Industries des Céréales, Lavoisier, Paris, 1996, p. 341.
[10] A.T. Aberle, W. Burchard, W. Vorweg, S. Radosta, Starch/Stärke 46 (1994) 329.
[11] B.F. Paschall, J.F. Foster, J. Polym. Sci. 9 (1952) 85.
[12] W. Banks, C.T. Greenwood, Starch and its Components, Edinburgh University Press, Edinburgh, 1975.
[13] C. Gérard, C. Barron, V. Planchot, P. Colonna, Carbohydrate Polymers 44 (2001) 19.
[14] W. Burchard, M. Schmidt, W.H. Stockmayer, Macromolecules 13 (1980) 1265.
[15] P.J. Flory, Principles of Polymer Chemistry, Cornell University Press, Ithaca, New York, 1953.
[16] P.G. de Gennes, Scaling concept in polymer chemistry, in: Cornell University Press, Ithaca, New York, 1979, p. 29.
[17] J.C. Le Guillou, J. Zinn-Justin, Phys. Rev. Lett. 39 (1977) 95.
[18] T. Kato, T. Katsuki, A. Takahashi, Macromolecules 17 (1984) 1726.
[19] Y. Nakanishi, T. Norisuye, A. Teramoto, S. Kitamura, Macromolecules 26 (1993) 4220.